

# Non-oscillating Early Dark Energy and Quintessence from $\alpha$ -Attractors

Lucy Brissenden, Konstantinos Dimopoulos and Samuel Sánchez López

Consortium for Fundamental Physics, Physics Department,  
Lancaster University, Lancaster LA1 4YB, United Kingdom.

E-mail: [l.brissenden@lancaster.ac.uk](mailto:l.brissenden@lancaster.ac.uk), [k.dimopoulos1@lancaster.ac.uk](mailto:k.dimopoulos1@lancaster.ac.uk),  
[s.sanchezlopez@lancaster.ac.uk](mailto:s.sanchezlopez@lancaster.ac.uk)

**Abstract.** Early dark energy (EDE) is one of the most promising possibilities in order to resolve the Hubble tension: the discrepancy between early and late-Universe measurements of the Hubble constant. In this paper we propose a model of a scalar field which can explain both EDE and late Dark Energy (DE) in a joined manner without additional fine-tuning. The field features kinetic poles as with  $\alpha$ -attractors. Our model provides an injection of EDE near matter-radiation equality, and redshifts away shortly after via free-fall, later refreezing to become late-time DE at the present day. Using reasonable estimates of the current constraints on EDE from the literature, we find that the parameter space is narrow but viable. As such our model is readily falsifiable. In contrast to other work in EDE, our model is non-oscillatory, which causes its decay to be faster than that of the usual oscillatory EDE, thereby achieving better agreement with observations.

---

## Contents

<b>1</b>	<b>Introduction</b>	<b>1</b>
1.1	The Hubble tension	2
1.2	Early Dark Energy	2
1.3	$\alpha$ -attractors	3
1.4	Quintessence	4
<b>2</b>	<b>The Model</b>	<b>5</b>
2.1	Lagrangian and Field Equations	5
2.2	Shape of Potential and Expected Behaviour	5
2.3	Asymptotic forms of the scalar potential	5
2.3.1	Expected Field Behaviour	7
2.4	Tuning requirements	8
<b>3</b>	<b>Numerical Simulation</b>	<b>9</b>
<b>4</b>	<b>Results and analysis</b>	<b>11</b>
4.1	Parameter Space	11
4.2	Field Behaviour	13
<b>5</b>	<b>Initial Conditions</b>	<b>14</b>
<b>6</b>	<b>Conclusions</b>	<b>19</b>
<b>A</b>	<b>Quintessential Inflation</b>	<b>20</b>

---

## 1 Introduction

In the last few decades cosmological observations of the early and late Universe have converged into a broad understanding of the history of our Universe from the very first seconds of its existence until today. Thus, cosmology has developed a standard model called the concordance model, or in short  $\Lambda$ CDM.

However, the latest data might imply that the celebrated  $\Lambda$ CDM model is not that robust after all. In particular, there is a  $5\text{-}\sigma$  discrepancy between the measurements of the current expansion rate, the Hubble constant  $H_0$ , as inferred by early Universe observations compared with late Universe observations. This Hubble tension has undermined our confidence in  $\Lambda$ CDM and as such it is investigated intensely at present.

In this work we study a toy model that can simultaneously solve the Hubble tension and explain the current accelerated expansion with no more tuning than in  $\Lambda$ CDM. Our model introduces a scalar field which plays both the role of early dark energy (EDE) and quintessence. In contrast to most other works in the literature which consider scalar fields as EDE, ours is not an oscillating scalar field.

We use natural units with  $c = \hbar = 1$ , the reduced Planck mass  $m_{\text{P}} = 1/\sqrt{8\pi G} = 2.43 \times 10^{18}\text{GeV}$  and consider a positive signature metric  $(-1, +1, +1, +1)$  throughout the present work.

## 1.1 The Hubble tension

Measurements in observational cosmology can broadly be classified into two groups. These are measurements of quantities which depend only on the early-time history of our Universe (such as the cosmic microwave background (CMB) radiation at redshift  $z \simeq 1100$ , or Baryon Acoustic Oscillations (BAO)) and measurements of quantities which depend on present-day observations (the primary example of this is the cosmic distance ladder, which measures the redshift of observable astrophysical objects such as Cepheid stars and type-1a supernovae, at redshift  $z = \mathcal{O}(1)$ ).

The value of the Hubble constant  $H_0$  can in principle be inferred from both early and late-time measurements. However, it has been found that while early-time measurements are in good agreement with each other, they disagree with current late-time data. Latest analysis of the CMB temperature anisotropies’ data gives the value inferred from Planck satellite [1],

$$H_0 = 67.44 \pm 0.58 \text{ km s}^{-1}\text{Mpc}^{-1}, \quad (1.1)$$

and a distance scale measurement using Cepheid-SN 1a data from the SH0ES collaboration [2] as

$$H_0 = 73.04 \pm 1.04 \text{ km s}^{-1}\text{Mpc}^{-1}. \quad (1.2)$$

This is a  $5\sigma$  tension which includes estimates of all systematic errors and which the SH0ES team conclude has “no indication of arising from measurement uncertainties or analysis variations considered to date”. It is becoming increasingly apparent with successive measurements that this tension is likely to have a theoretical resolution [3–6], which can have many possible sources [7, 8] but increasingly favours early-time modifications [9, 10].

## 1.2 Early Dark Energy

One proposed class of solutions to the Hubble tension is models of Early Dark Energy (EDE), whose early works include references [11–14], followed by many others, e.g. see Refs. [7, 15–40]. These involve an injection of energy in the dark energy sector at around the time of matter-radiation equality, which then dilutes or otherwise decays away faster than the background energy density, such that it becomes negligible before it can be detected in the CMB. As briefly reviewed below, such models result in a slight change in the expansion history of the Universe, bumping up the value of the Hubble parameter at the present day.

It has previously been concluded [3, 7, 8] that EDE models are most likely to source a theoretical resolution to the Hubble tension. One reason for this is that EDE can effect substantial modifications to  $H_0$  without significant effect on other cosmological parameters which are tightly constrained by observations.<sup>1</sup> In particular, EDE models can be incorporated into existing scalar-field models of inflation and late-time dark energy; one example of the latter is the model detailed in this work.

However, precisely because EDE models exist so close in time to existing observational data, they have significant constraints; the primary consideration being that EDE must be subdominant at all times and must decay away fast enough to be essentially negligible at the time of last scattering translating to a redshift rate that is faster than radiation [12]. So far, in previous works in EDE, this has been achieved by considering first or second-order phase transitions (e.g. [27], [33]). These abrupt events might have undesirable side-effects such

---

<sup>1</sup>Models which modify other cosmological parameters are often unable to reconcile their changes with current observational constraints on said parameters (see Ref. [7] for a comprehensive review).

as inhomogeneities from bubble collisions or topological defects. Other proposed models [7, 11, 12, 27–34] typically feature oscillatory behaviour to achieve the rapid decay rate necessary for EDE to be negligible at last scattering. As with the original proposal in Ref. [11], the EDE field is taken to oscillate around its Vacuum Expectation Value (VEV) in a potential minimum which is tuned to be of order higher than quartic. As a result, its energy density decays on average as  $\propto a^{-n}$ , with  $4 < n < 6$ . In contrast, in our model, the EDE scalar field experiences a period of kinetic domination, where the field is in non-oscillatory free-fall and its density decreases as  $\propto a^{-6}$ , exactly rather than approximately.

Before continuing, we briefly explain how EDE manages to increase the value of  $H_0$  as from CMB observations. Measurements of the CMB temperature anisotropies provide very tight constraints on the cosmological parameters. One would therefore think that this severely limits models which alter the Universe content and dynamics at this time. However, there are certain classes of models for which this is not the case. These are models that affect both the Hubble parameter and  $r_s$ , the comoving sound horizon<sup>2</sup> (in this case during the drag epoch, shortly after recombination), given by

$$r_s = \int_{z_d}^{\infty} \frac{c_s(z)}{H(z)} dz, \quad (1.3)$$

where  $c_s(z)$  is the sound speed and  $H(z)$  is the Hubble parameter, both as a function of redshift.

An additional amount of dark energy in the Universe increases the total density, which in turn increases the Hubble parameter because of the Friedmann equation  $\rho \propto H^2$ . Therefore, EDE considers such a brief increase at or before decoupling, which lowers the value of the sound horizon because it increases  $H(z)$  in Eq. (1.3). However, there is a way to avoid this being evident in and therefore disproved by current CMB measurements. This is because BAO and CMB measurements do not constrain the value of the sound horizon directly.

For example, BAO measurements do not constrain the sound horizon alone, but the combination  $H(z)r_s$  [41]. The observations of the Planck satellite measure the quantity  $\theta_* \equiv \frac{r_s}{D_*}$  [42], the angular scale of the sound horizon; given by ratio of the comoving sound horizon to the angular diameter distance at which we observe fluctuations. Both of these measurements entail an assumption of  $\Lambda$ CDM cosmology and can be shown to be equally constrained by other models, provided that they make only small modifications which simultaneously lower the value of  $r_s$  and increase  $H_0$ .

EDE may have a significant drawback, however, in that it does not alleviate the  $\sigma_8$  tension (associated with matter clustering) and may in fact exacerbate it [3, 43–45]. As with many others, our model does not attempt to solve this problem.

### 1.3 $\alpha$ -attractors

Our model unifies EDE with late DE in the context of  $\alpha$ -attractors. An earlier attempt for such unification in the same theoretical context can be seen in Ref. [34]. However, this proposal is also of oscillatory EDE.

$\alpha$ -attractors [46–54], which appear naturally in conformal field theory or supergravity theories, are a class of models whose inflationary predictions continuously interpolate between those of chaotic inflation [55] and those of Starobinsky [56] and Higgs inflation [57]. In

---

<sup>2</sup>This is the characteristic scale of BAO, typically approximately proportional to the value of the cosmological horizon at that point by  $r_s = \frac{1}{\sqrt{3}}r_H$  assuming spatial flatness.

supergravity, introducing curvature to the internal field-space manifold can give rise to a non-trivial Kähler metric, which results in kinetic poles for some of the scalar fields of the theory. The free parameter  $\alpha$  is inversely proportional to said curvature. It is also worth clarifying what is meant by the word “attractor”. It is not only used in the usual sense (*i.e.*, field trajectories during inflation flowing to a unique one, regardless of the initial conditions), but also to refer to the fact that the inflationary predictions are largely insensitive of the specific characteristics of the model under consideration. Such an attractor behaviour is seen for sufficiently large curvature (small  $\alpha$ ) in the internal field-space manifold.

In practical terms, the scalar field has a non-canonical kinetic term, featuring two poles, which the field cannot transverse. To aid our intuition, the field can be canonically normalised via a field redefinition, such that the finite poles for the non-canonical field are transposed to infinity for the canonical one. As a result, the scalar potential is “stretched” near the poles, resulting in two plateau regions, which are useful for modelling inflation, see *e.g.* Refs. [58–63] or quintessence [64], or both, in the context of quintessential inflation [64–66].

Following the standard recipe, we introduce two poles at  $\varphi = \pm\sqrt{6\alpha} m_P$  by considering the Lagrangian

$$\mathcal{L} = \frac{-\frac{1}{2}(\partial\varphi)^2}{\left(1 - \frac{\varphi^2}{6\alpha m_P^2}\right)^2} - V(\varphi), \quad (1.4)$$

where  $\varphi$  is the non-canonical scalar field and we use the short-hand notation  $(\partial\varphi)^2 \equiv g^{\mu\nu}\partial_\mu\varphi\partial_\nu\varphi$ . We then redefine the non-canonical field in terms of the canonical scalar field  $\phi$  as

$$d\phi = \frac{d\varphi}{1 - \frac{\varphi^2}{6\alpha m_P^2}} \quad \Rightarrow \quad \varphi = m_P\sqrt{6\alpha} \tanh\left(\frac{\phi}{\sqrt{6\alpha} m_P}\right). \quad (1.5)$$

It is obvious that the poles  $\varphi = \pm\sqrt{6\alpha}$  are transposed to infinity.

In terms of the canonical field, the Lagrangian now reads

$$\mathcal{L} = -\frac{1}{2}(\partial\phi)^2 - V(\phi). \quad (1.6)$$

#### 1.4 Quintessence

“Early” Dark Energy is so named in order to make it distinct from “late” Dark Energy, which is the original source of the name (and often just called Dark Energy (DE)). In cosmological terms the latter is just beginning to dominate the Universe at present, making up approximately 70% of the Universe’s energy density [67]. This is the mysterious unknown substance that is responsible for the current accelerating expansion of the Universe and has equation-of-state (barotropic) parameter of  $w = -1.03 \pm 0.03$  [1].

Late DE that is due to an (as-yet-undiscovered) scalar field is called *quintessence* [68], so-named because it is the “fifth element” making up the content of the Universe<sup>3</sup>. In this case, the Planck-satellite bound on the barotropic parameter of DE is  $-1 \leq w < -0.95$  [1]. Quintessence is distinct from other explanations for DE because a scalar field has a variable barotropic parameter and can therefore exhibit completely different behaviour in different periods of the Universe’s history. In order to get it to look like late-time DE, a scalar field should be dominated by its potential density, making its barotropic parameter sufficiently

<sup>3</sup>After baryonic matter, dark matter, photons and neutrinos.

close to  $-1$ . It is useful to consider the CPL parametrization, which is obtained by Taylor expanding  $w(z)$  near the present as [69, 70]

$$w(z) = w_0 + w_a \frac{z}{z+1}, \quad (1.7)$$

where  $w_a \equiv -(dw/da)_0$ . The Planck satellite observations impose the bounds [1]

$$\begin{aligned} -1 &\leq w < -0.95 \\ w_a &= -0.29^{+0.32}_{-0.26}. \end{aligned} \quad (1.8)$$

## 2 The Model

### 2.1 Lagrangian and Field Equations

Consider a potential of the form

$$\begin{aligned} V(\varphi) &= V_X \exp\left(-\lambda e^{\kappa\varphi/m_P}\right), \\ \text{with } V_\Lambda &\equiv \exp\left(-\lambda e^{\kappa\sqrt{6\alpha}}\right) V_X, \end{aligned} \quad (2.1)$$

where  $\alpha, \kappa, \lambda$  are dimensionless model parameters,  $V_X$  is a constant energy density scale and  $\varphi$  is the non-canonical scalar field with kinetic poles given by the typical alpha attractors form (see [50]) with Lagrangian density given by Eq. (1.4).<sup>4</sup> In the above,  $V_\Lambda$  is the vacuum density at present. To assist our intuition, we switch to the canonically normalised (canonical) scalar field  $\phi$ , using the transformation in Eq. (1.5). In terms of the canonical scalar field, the Lagrangian density is then given by Eq. (1.6), where the scalar potential is

$$V(\phi) = \exp\left(\lambda e^{\kappa\sqrt{6\alpha}}\right) V_\Lambda \exp\left[-\lambda e^{\kappa\sqrt{6\alpha} \tanh(\phi/\sqrt{6\alpha} m_P)}\right]. \quad (2.2)$$

As usual, the Klein-Gordon equation of motion for the homogeneous canonical field is

$$\ddot{\phi} + 3H\dot{\phi} + V'(\phi) = 0, \quad (2.3)$$

where the dot and prime denote derivatives with respect to the cosmic time and the scalar field respectively, and we assumed that the field was homogenised by inflation, when the latter overcame the horizon problem.

### 2.2 Shape of Potential and Expected Behaviour

Henceforth we will discuss the behaviour of the field in terms of the variation, i.e. movement in field space, of the canonical field.

### 2.3 Asymptotic forms of the scalar potential

We are interested in two limits for the potential above:  $\phi \rightarrow 0$  ( $\varphi \rightarrow 0$ ) and  $\phi \rightarrow +\infty$  ( $\varphi \rightarrow \sqrt{6\alpha} m_P$ ). The first limit would correspond to matter-radiation equality. In this limit, the potential is

---

<sup>4</sup>The model parameter is  $V_X$  and not  $V_\Lambda$ , the latter being generated by  $V_X$  and the remaining model parameters as shown in Eq. (2.1).

$$V_{\text{eq}} \simeq \exp\left[\lambda(e^{\kappa\sqrt{6\alpha}} - 1)\right] V_{\Lambda} \exp(-\kappa\lambda\phi_{\text{eq}}/m_{\text{P}}), \quad (2.4)$$

where the subscript ‘eq’ denotes the time of matter-radiation equality when the field unfreezes. It is assumed that the field was originally frozen there. We discuss and justify this assumption in Sec. 5. After unfreezing, it is considered that the field has not varied much, for the above approximation to hold, i.e.

$$0 \lesssim \phi_{\text{eq}} \ll \sqrt{6\alpha}m_{\text{P}}. \quad (2.5)$$

This is a reasonable assumption given that the field begins shortly before matter-radiation equality frozen at the origin, unfreezing at some point during this time<sup>5</sup>.

At large  $\phi$  ( $\phi \rightarrow \infty$ ), the non-canonical field is near the kinetic pole ( $\varphi \rightarrow \sqrt{6\alpha}m_{\text{P}}$ ). Then the potential in this limit is

$$V_0 \simeq V_{\Lambda} \left[ 1 + 2\kappa\lambda e^{\kappa\sqrt{6\alpha}}\sqrt{6\alpha} \exp\left(-\frac{2\phi_0}{\sqrt{6\alpha}m_{\text{P}}}\right) \right], \quad (2.6)$$

which, even for sub-Planckian total field excursion in  $\phi$ , should be a good approximation for sufficiently small  $\alpha$ . The subscript ‘0’ denotes the present time.<sup>6</sup>

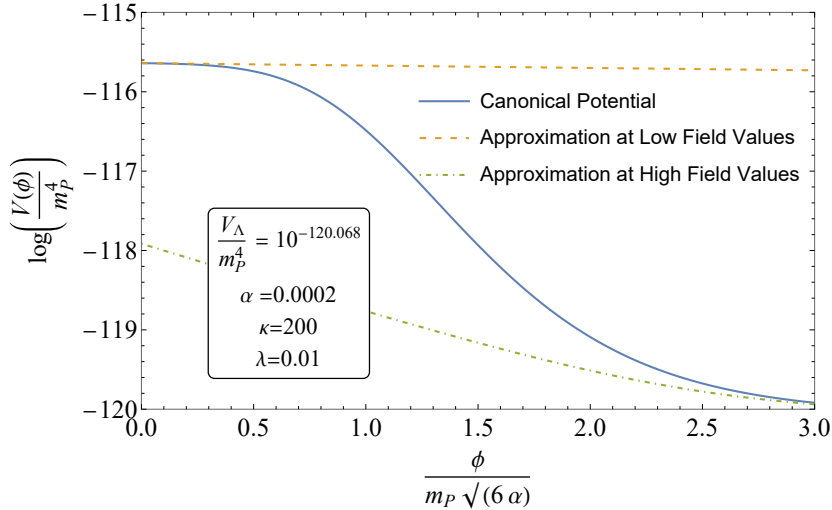


**Figure 1:** Graph of the canonical potential and its two approximations for small and large field values, given in Eqs. (2.4) and (2.6) respectively. These approximations are useful because they are simple exponential potentials with known attractors, so we know the type of behaviour the field should exhibit when each approximation is valid. It can be readily seen that, after leaving the origin the field jumps off a potential plateau and is free-falling as a result.

<sup>5</sup>There is no suggestion in the EDE literature [7, 11, 12, 27–34] that the field has to unfreeze at any particular time, as long as it does not grow to larger than the allowed fraction and its energy density is essentially negligible by the time of decoupling.

<sup>6</sup>Note that, as the field becomes very large, the potential approaches the positive constant  $V_{\Lambda}$ , which corresponds to non-zero vacuum density with  $w = -1$ , as in  $\Lambda$ CDM. Thus, our model outperforms pure quintessence (with  $-1 < w < -0.95$  [1]), which can push  $H_0$  to lower instead of higher values [71, 72].

The above approximations describe well the scalar potential near equality and the present time, as shown in Fig. 1. As we explain below, in between these regions, the scalar field free-falls and becomes oblivious of the scalar potential as the term  $V'(\phi)$  in its equation of motion (2.3) becomes negligible.

### 2.3.1 Expected Field Behaviour

Here we explain the rationale behind the mechanism envisaged. We make a number of crude approximations, which enable us to follow the evolution of the scalar field, but which need to be carefully examined numerically. We do so in the next section.

First, we consider that originally the field is frozen at zero (for reasons explained in Sec. 5). Its energy density is such that it remains frozen there until equality, when it thaws following the appropriate exponential attractor, since  $V_{\text{eq}}$  in Eq. (2.4) is approximately exponential [73]. Assuming that this is the subdominant attractor requires that the strength of the exponential is [74, 75]

$$Z \equiv \kappa\lambda > \sqrt{3}. \quad (2.7)$$

The subdominant exponential attractor dictates that the energy density of the rolling scalar field mimics the dominant background energy density. Thus, the density parameter of the field is constant, given by the value [73–75]

$$\Omega_\phi^{\text{eq}} \simeq \frac{3}{Z^2} = \frac{3}{(\kappa\lambda)^2} < 1 \quad (2.8)$$

This provides an estimate of the moment when the originally frozen scalar field, unfreezes and begins rolling down its potential. Unfreezing happens when  $\Omega_\phi$  (which is growing while the field is frozen, because the background density decreases with the expansion of the Universe) obtains the above value.

However, after unfreezing, the field soon experiences the full  $\exp(\exp)$  steeper than exponential potential so, it does not follow the subdominant attractor any more but it free-falls,<sup>7</sup> such that its density scales as  $\rho_\phi \simeq \frac{1}{2}\dot{\phi}^2 \propto a^{-6}$ , until it refreezes at a larger value  $\phi_F$ . This value is estimated as follows.

In free-fall, the slope term in the equation of motion (2.3) of the field is negligible, so that the equation is reduced to  $\ddot{\phi} + 3H\dot{\phi} \simeq 0$ , where  $H = 2/3t$  after equality. The solution is

$$\phi(t) = \phi_{\text{eq}} + \frac{C}{t_{\text{eq}}} \left( 1 - \frac{t_{\text{eq}}}{t} \right), \quad (2.9)$$

where  $C$  is an integration constant. From the above, it is straightforward to find that  $\dot{\phi} = Ct^{-2}$ . Thus, the density parameter at equality is

$$\begin{aligned} \Omega_\phi^{\text{eq}} &= \frac{\rho_\phi}{\rho} \Big|_{\text{eq}} = \frac{\frac{1}{2}C^2 t_{\text{eq}}^{-4}}{\frac{4}{3}(m_P t_{\text{eq}})^2} = \frac{3}{8} \frac{C^2}{(m_P t_{\text{eq}})^2} \\ \Rightarrow C &= \sqrt{\frac{8}{3}\Omega_\phi^{\text{eq}}} m_P t_{\text{eq}} = \frac{\sqrt{8}}{\kappa\lambda} m_P t_{\text{eq}}, \end{aligned} \quad (2.10)$$

where we used Eq. (2.8),  $\rho_\phi \simeq \frac{1}{2}\dot{\phi}^2$  and that  $\rho = 1/6\pi Gt^2 = \frac{4}{3}(m_P/t)^2$ . Thus, the field freezes at the value

$$\phi_0 = \phi_{\text{eq}} + C/t_{\text{eq}} = \phi_{\text{eq}} + \frac{\sqrt{8}}{\kappa\lambda} m_P, \quad (2.11)$$

---

<sup>7</sup>i.e. its energy density is dominated by its kinetic energy density only.

where we considered that  $t_{\text{eq}} \ll t_{\text{freeze}} < t_0$ .

Using that  $t_{\text{eq}} \sim 10^4$  y and  $t_0 \sim 10^{10}$  y, we can estimate

$$\frac{V_{\text{eq}}}{V_0} \simeq \frac{\Omega_{\phi}^{\text{eq}} \rho_{\text{eq}}}{0.7 \rho_0} \simeq \frac{30}{7(\kappa\lambda)^2} \left( \frac{t_0}{t_{\text{eq}}} \right)^2 \simeq \frac{3}{7(\kappa\lambda)^2} \times 10^{13}. \quad (2.12)$$

Now, from Eqs. (2.4) and (2.6) we find

$$\frac{V_{\text{eq}}}{V_0} \simeq \frac{e^{\lambda(e^{\kappa\sqrt{6\alpha}}-1)} \exp(-\kappa\lambda\phi_{\text{eq}}/m_P)}{1 + 2\kappa\lambda e^{\kappa\sqrt{6\alpha}}\sqrt{6\alpha} \exp(-2\phi_0/\sqrt{6\alpha}m_P)}. \quad (2.13)$$

In view of Eqs. (2.5) and (2.11), the above can be written as

$$\frac{V_{\text{eq}}}{V_0} \simeq \frac{e^{\lambda(e^{\kappa\sqrt{6\alpha}}-1)}}{1 + 2\kappa\lambda e^{\kappa\sqrt{6\alpha}}\sqrt{6\alpha} e^{-2\sqrt{8}/\kappa\lambda\sqrt{6\alpha}}}. \quad (2.14)$$

Taking  $\Omega_{\phi}^{\text{eq}} \simeq 0.1$  as required by EDE, Eq. (2.8) suggests

$$\kappa\lambda \simeq \sqrt{30}. \quad (2.15)$$

Combining this with Eq. (2.12) we obtain

$$e^{\frac{\sqrt{30}}{\kappa}(e^{\kappa\sqrt{6\alpha}}-1)} \sim 10^{12}/7, \quad (2.16)$$

where we have ignored the 2nd term in the denominator of the right-hand-side of Eq. (2.14).

From the above we see that,  $\kappa$  is large when  $\alpha$  is small. Taking, as an example,  $\alpha = 0.01$  we obtain  $\kappa \simeq 18$  and  $\lambda \simeq 0.30$  (from Eq. (2.15)). With these values, the second term in the denominator of the right-hand-side of Eq. (2.14), which was ignored above, amounts to the value 3.2. This forces a correction to the ratio  $V_{\text{eq}}/V_0$  of order unity, which means that the order-of-magnitude estimate in Eq. (2.16) is not affected.

Using the selected values, Eq. (2.11) suggests that the total excursion of the field is

$$\Delta\phi = \phi_0 - \phi_{\text{eq}} = \frac{\sqrt{8}}{\kappa\lambda} m_P \simeq 0.5 m_P, \quad (2.17)$$

i.e. it is sub-Planckian. In the approximation of Eq. (2.4), we see that the argument of the exponential becomes  $\kappa\lambda\Delta\phi/m_P \simeq 2.7 > 1$ , where we used Eq. (2.15). This means that the approximation breaks down and the exp(exp) potential is felt as considered, as depicted also in Fig. 1.

For small  $\alpha$  the eventual exponential potential in Eq. (2.6) is steep, which suggests that field rushes towards the minimum at infinity and the barotropic parameter is  $w \approx -1$  because the potential is dominated by the constant  $V_{\Lambda}$ .

## 2.4 Tuning requirements

Our model addresses in a single shot two cosmological problems: firstly, the Hubble tension between inferences of  $H_0$  using early and late-time data; and secondly, the reason for the late-time accelerated expansion of the Universe; late DE. However, it is subject to some tuning. Namely, the two free parameters  $\kappa$  and  $\lambda$ , the intrinsic field-space curvature dictated by  $\alpha$ , and the scale of the potential introduced by  $V_{\Lambda}$ .

As we have seen  $\kappa$  and  $\lambda$  seem to take natural values, not too far from order unity. Regarding  $\alpha$  we only need that it is small enough to lead to rapid decrease of the exponential contribution in the scalar potential in Eq. (2.6), leaving the constant  $V_\Lambda$  to dominate at present. We show in the next section that  $\alpha \sim 10^{-4}$  is sufficient for this task. This leaves  $V_\Lambda$  itself. The required tuning of this parameter is given by  $V_\Lambda = \left(\frac{H_0^{\text{Planck}}}{H_0^{\text{SHOES}}}\right)^2 V_\Lambda^{\text{Planck}}$ , where  $V_\Lambda^{\text{Planck}}$  is given by the Planck 2018 [1] estimate of  $\rho_0$ , the density today, multiplied by  $\Omega_\Lambda$ , the estimate of the density parameter of dark energy today, i.e.  $V_\Lambda^{\text{Planck}} = \Omega_\Lambda \rho_0$ . Since  $\left(\frac{H_0^{\text{Planck}}}{H_0^{\text{SHOES}}}\right)^2 \simeq \left(\frac{67.44}{73.04}\right)^2 = 0.8525$  we see that the required fine-tuning of our  $V_\Lambda$  is not different from the fine-tuning introduced in  $\Lambda$ CDM, but, in contrast to  $\Lambda$ CDM, our proposal addresses two cosmological problems; not only late DE but also the Hubble tension.<sup>8</sup>

### 3 Numerical Simulation

In order to numerically solve the dynamics of the system, it is enough to solve for the scale factor  $a(t)$ , the field  $\phi(t)$  and the background fluid densities  $\rho_m(t)$  and  $\rho_r(t)$ , as every other quantity depends on these. They are governed by the Friedmann equations, the Klein-Gordon equation and the continuity equations respectively. Of course, the Klein-Gordon equation is a second order ODE, while the continuity equations are first order so that we need the initial value and velocity of  $\phi$  and just the initial value of  $\rho_m$  and  $\rho_r$  as initial conditions. As described above, the field starts frozen and unfreezes around matter-radiation equality. Effectively, this means using  $\phi_{\text{ini}} = 0$  and  $\dot{\phi}_{\text{ini}} = 0$  as initial conditions, a few e-folds before matter-radiation equality, while the initial radiation and matter energy densities are chosen to satisfy the bounds obtained by Planck [1] at matter-radiation equality, *i.e.*,  $\rho_m(t_{\text{eq}}) = \rho_r(t_{\text{eq}}) = 1.27 \times 10^{-110} m_{\text{P}}^4$ .

For convenience, we rewrite the equations in terms of the logarithmic energy densities  $\tilde{\rho}_m(t) = \ln(\rho_m(t)/m_{\text{P}}^4)$  and  $\tilde{\rho}_r(t) = \ln(\rho_r(t)/m_{\text{P}}^4)$ . Plugging the first Friedmann equation in the Klein-Gordon equation, gives

$$\ddot{\phi}(t) + \frac{\sqrt{3\rho(t)}}{m_{\text{P}}} \dot{\phi}(t) + \frac{dV}{d\phi} = 0, \quad (3.1)$$

$$\dot{\tilde{\rho}}_m(t) + \frac{\sqrt{3\rho(t)}}{m_{\text{P}}} = 0, \quad (3.2)$$

$$\dot{\tilde{\rho}}_r(t) + \frac{4}{3} \frac{\sqrt{3\rho(t)}}{m_{\text{P}}} = 0, \quad (3.3)$$

where  $3m_{\text{P}}^2 H^2(t) = \rho(t) = [\exp(\tilde{\rho}_m(t)) + \exp(\tilde{\rho}_r(t))]m_{\text{P}}^4 + \rho_\phi(t)$  and  $\rho_\phi(t) = K(\phi(t)) + V(\phi(t))$  where  $K(\phi(t)) = \frac{1}{2}(\dot{\phi}(t))^2$  and  $V(\phi(t))$  is given by Eq. (2.2).

As mentioned above, we assume the field to be frozen at an ESP, such that it could have been the inflaton or a spectator field at earlier times. The time of unfreezing is then controlled only by the parameters of the model's potential.<sup>9</sup> The densities of matter and radiation are scaled back to find some initial conditions at some arbitrary redshift,  $z_{\text{ini}} = 10^4$ , before equality.

<sup>8</sup>In our simulations we use  $V_\Lambda = 10^{-120.068} m_{\text{P}}^4$  as assumed also in Fig. 1.

<sup>9</sup> Although we could use an estimate for the initial time, it turns out that it makes no difference to the numerical results or the behaviour of the field and simply offsets the differential equations.

Initial Densities	Calculation	Value
Matter	$\rho_m = 3\Omega_{m,0}^{\text{Planck}} m_P^2 (H_0^{\text{SHOES}})^2$	$3.84 \times 10^{-121} m_P^4$
Radiation	$\frac{\pi^2}{30} g_*(T_{\text{CMB},0}^{\text{Planck}})^4$	$9.56 \times 10^{-125} m_P^4$

**Table 1:** Table of present-day densities, where the present matter density parameter is  $\Omega_{m,0}^{\text{Planck}} = 0.3111$ ,  $T_{\text{CMB},0}^{\text{Planck}} = 2.7255$  K and the effective relativistic degrees of freedom of radiation are  $g_* = 3.36$ , calculated by taking the photon and neutrino contribution into account (see section 5 of [76]).

Variable	Initial Value	Source
Redshift	$z_{\text{initial}} = 10^4$	chosen to be shortly before matter-radiation equality
Time	$t_{\text{ini}} = 0.1 m_P^{-1}$	chosen to be close to zero (see footnote 9)
Field Value	$\phi(t_{\text{ini}}) = 0$	simplified initial conditions
Rate of change of Field Value	$\dot{\phi}(t_{\text{ini}}) = 0$	simplified initial conditions
Density of Matter	$\rho_m(t_{\text{ini}}) = 3.84 \times 10^{-109} m_P^4$	$\rho_m(t_0)_{\text{Planck}} (z_{\text{ini}} + 1)^3$
Density of Radiation	$\rho_r(t_{\text{ini}}) = 1.24 \times 10^{-108} m_P^4$	$\rho_r(t_0)_{\text{Planck}} (z_{\text{ini}} + 1)^4$
E-folds elapsed	$N_{\text{ini}} = 0$	chosen for convenience

**Table 2:** Table detailing the initial conditions for the differential equations.

The differential solver records three “events” during solving: matter-radiation equality, triggered by the obvious condition; decoupling, triggered by the total energy density taking the correct value; and the present day, triggered by the field making up the correct fraction of the total energy density (as estimated by the Planck satellite [1]). These values are saved to an association so that they can later be searched to identify points which fulfill the necessary constraints, in order to find a viable parameter space. Once the final event is recorded, the solver is terminated.

Event	Criteria	Justification
Matter-Radiation Equality	$\rho_m(t_{\text{eq}}) = \rho_r(t_{\text{eq}})$	Theoretical Definition
Last Scattering	$\rho_m(t_{\text{ls}}) = 4.98 \times 10^{-112} m_P^4$	Extrapolation from $\Lambda$ CDM initial conditions (see Table 2) using Planck results $\rho_m(z_{\text{eq}})$ with $z_{\text{eq}} = 1089.80$ [1]
Present Day	$\Omega_\phi = 0.6889$	Planck data [1]

**Table 3:** Table of events recorded during the numerical solving of equations and how.

If a field point does not meet the conditions for the final event (i.e. the present day), this indicates that the field began the simulation as the dominant component and will never reach the correct energy density. The point is thrown away. Finally, reasonable observational and theoretical constraints to the parameter space are applied to the data collected, which are outlined in Table 4.

Parameter to be constrained	Source	Description	Constraint
Density parameter of the field at equality	EDE literature [29]	Upper limit governed by the maximum value that does not impede structure formation; lower limit is so that EDE actually has an effect	$0.015 \leq \Omega_\phi^{\text{eq}} < 0.107$
Density parameter of the field at Last Scattering	EDE literature [12]	This is the upper limit that ensures EDE cannot currently be detected in the CMB	$\Omega_\phi^{\text{ls}} < 0.015$
Density parameters of the field at Last Scattering and Equality	Theoretical	Achieves desired behaviour of the field	$\Omega_\phi^{\text{eq}} > \Omega_\phi^{\text{ls}}$
Density parameter of the field today	Planck 2018 [1]	Observational constraint	$0.6833 \leq \Omega_\phi^0 \leq 0.6945$
Barotropic parameter of the field today	Planck 2018	Observational constraint	$-1 \leq w_\phi^0 \leq -0.95$
Running of the barotropic parameter today	Planck 2018 [1]	Observational constraint	$-0.55 \leq w_\phi^a \leq 0.03$
Hubble constant	SH0ES 2021 [2]	Observational constraint	$72.00 \leq \frac{H_0}{\text{km s}^{-1} \text{Mpc}^{-1}} \leq 74.08$
Total Field Excursion	Theoretical	From analytical estimates, the total excursion of the field should ideally be sub-Planckian	$\phi_0 - \phi_{\text{eq}} < m_{\text{P}}$

**Table 4:** Table describing and justifying constraints used to identify the viable parameter space. In the above,  $w_\phi^a = -\left.\frac{dw_\phi}{da}\right|_0$ , c.f. Eq. (1.8).

## 4 Results and analysis

### 4.1 Parameter Space

As evident from Figs. 2, 3 and 4, we find that  $\kappa \sim 10^2$  and  $\lambda \sim 10^{-3}$ , which are rather reasonable values. In particular, the value of  $\kappa$  suggests that the mass-scale which suppresses the non-canonical field  $\varphi$  in the original potential in Eq. (2.1) is near the scale of grand unification  $\sim 10^{-2} m_{\text{P}}$ . Regarding the curvature of field space we find  $\alpha \sim 10^{-4}$ , which again is not unreasonable.

The viable parameter space suggests that  $\kappa\lambda > \sqrt{3}$ , which contradicts our assumption in Eq. (2.7). This implies that, unlike the analytics in Sec. 2.3.1, the field does not adopt the subdominant exponential scaling attractor but the slow-roll exponential attractor, which leads to domination [73, 75]. As the field thaws and starts following this attractor, the approximation in Eq. (2.4) breaks down as the field experiences the full  $\exp(\exp)$  potential, which is steeper than exponential (see Fig. 1). Consequently, instead of becoming dominant the field free-falls. This contradiction with our discussion in Sec. 2.3.1 is not very important.

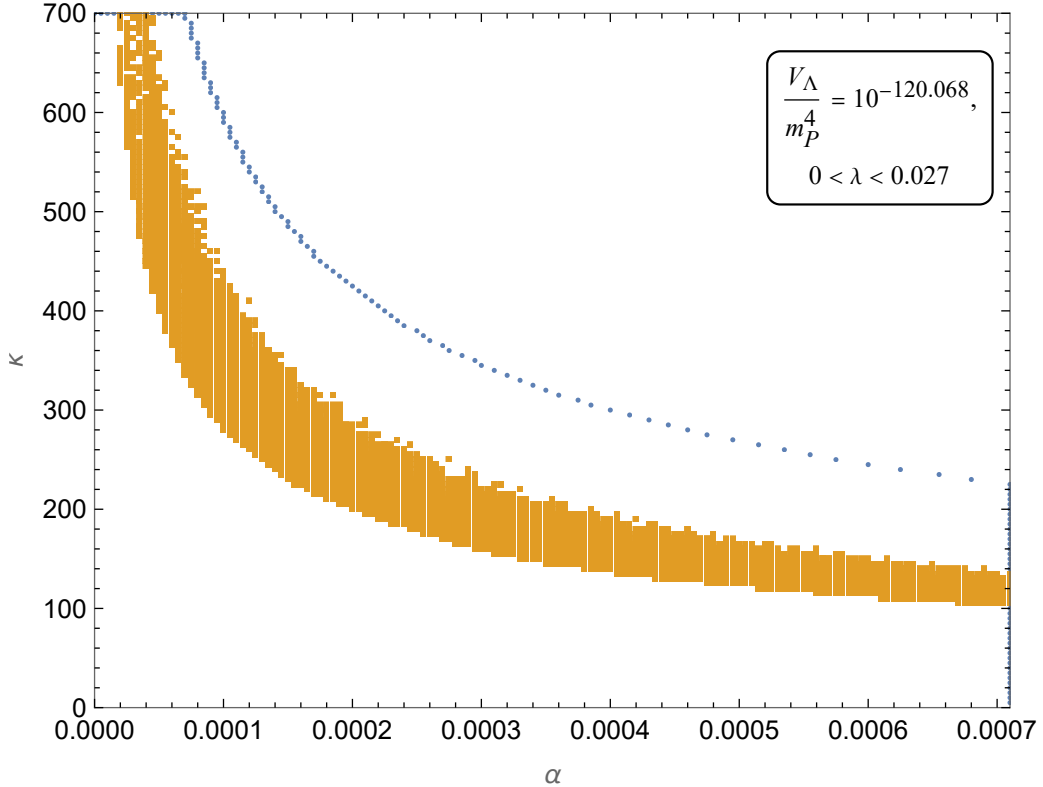


**Figure 2:** Parameter space slice in the  $\kappa - \alpha$  plane with  $0 < \lambda < 0.027$  and  $V_\Lambda = 10^{-120.068} m_P^4$ . The blue dotted line is the boundary of the region that produces non-inflationary results (see below), while the orange region is constituted by the successful points, *i.e.*, those for which the constraints detailed in Table 4 are satisfied. Note that the region bounded in blue is not equal to the range of the scan, which goes from  $0 \leq \kappa \leq 700$ ,  $0 \leq \alpha \leq 0.00071$ . This is because points with potential larger than a certain starting value result in the field beginning the simulation dominant, which means that the Universe goes into inflation which cannot terminate and will never meet the numerical end condition for the present day. These points are very close to the viable parameter space for these two parameters and therefore must be thrown away.

The existence of the scaling attractor provided an easy analytic estimate for the moment when the field unfreezes. It turns out that, because the scaling attractor has been substituted by the slow-roll attractor, the field unfreezes because its potential energy density becomes comparable to the total energy density, going straight into free-fall. It is much harder to analytically estimate when exactly this takes place, but the eventual result (free-fall) is the same.

The redshift of matter-radiation equality occurs earlier than usual at  $z_{\text{eq}} \simeq 4000$ . However, equality occurs well before last scattering,  $z_{\text{eq}} > z_{\text{ls}}$  and its redshift is only indirectly inferred by observations. In contrast, the redshift of last scattering is where we would expect it at  $z_{\text{ls}} \simeq 1087$ . Theoretical constraints suggest  $z_{\text{ls}} \simeq 1090$  [77], and the observations of the Planck satellite suggest  $z_{\text{ls}} = 1089.80 \pm 0.21$  [1].

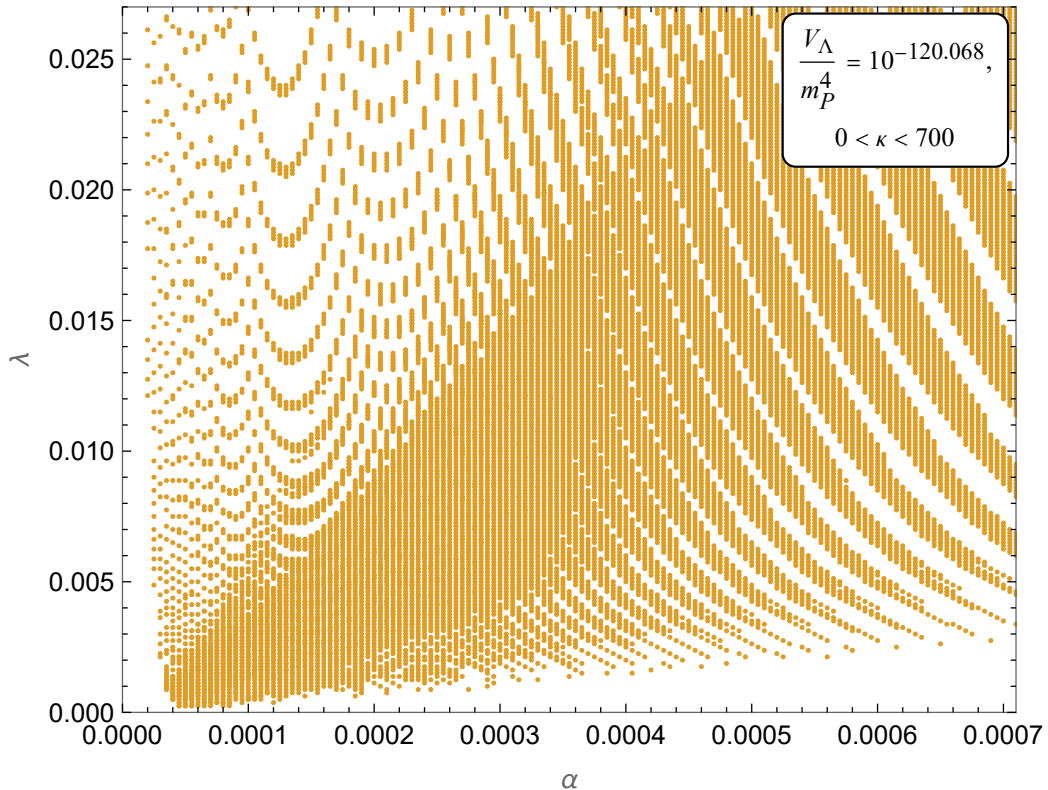


**Figure 3:** Parameter space slice in the  $\lambda - \alpha$  plane with  $0 < \kappa < 700$  and  $V_\Lambda = 10^{-120.068} m_P^4$ . The orange region is constituted by the successful points, *i.e.*, those for which the constraints detailed in Table 4 are satisfied.

## 4.2 Field Behaviour

The field behaves as expected, with the mild modification of the attractor solution at un-freezing (slow-roll instead of scaling), which leads to free-fall. The evolution is depicted in Figs. 5, 6, 7 and 8 for the example point at  $\alpha = 0.0005$ ,  $\kappa = 145$ ,  $\lambda = 0.008125$ , and  $V_\Lambda$  tuned to the SH<sub>0</sub>ES cosmological constant [2]. The observables obtained in this case (*i.e.* the values of  $H_0$ ,  $w_0$  and  $w_a$ ) are shown in Table 5. The behaviour of the Hubble parameter is a function of redshift as can be seen in Fig. 7.

As mentioned in Table 4, the maximum allowed value of the EDE density parameter at equality is just over 0.1. However, it is possible that this is too lenient a constraint because unlike the models for which this constraint was developed, our model has a true free-fall period, which means it redshifts away *exactly* as  $a^{-6}$  rather than below this rate as in oscillatory behaviour (see Figs. 5 and 8). A full MCMC analysis may provide a more accurate constraint for non-oscillatory models.

At present, the exponential contribution to the potential density in Eq. (2.6) is largely subdominant to  $V_\Lambda$ , so the contribution of the scalar field to the total density budget is almost constant, as in  $\Lambda$ CDM. Its barotropic parameter is, therefore,  $w_\phi \approx -1$  (see Fig. 5). Technically, it is not exactly -1 but its running is negligible, with the viable parameter space for  $w_a$  fitting easily within the constraint in Eq. (1.8) by some ten orders of magnitude (see Table 5).

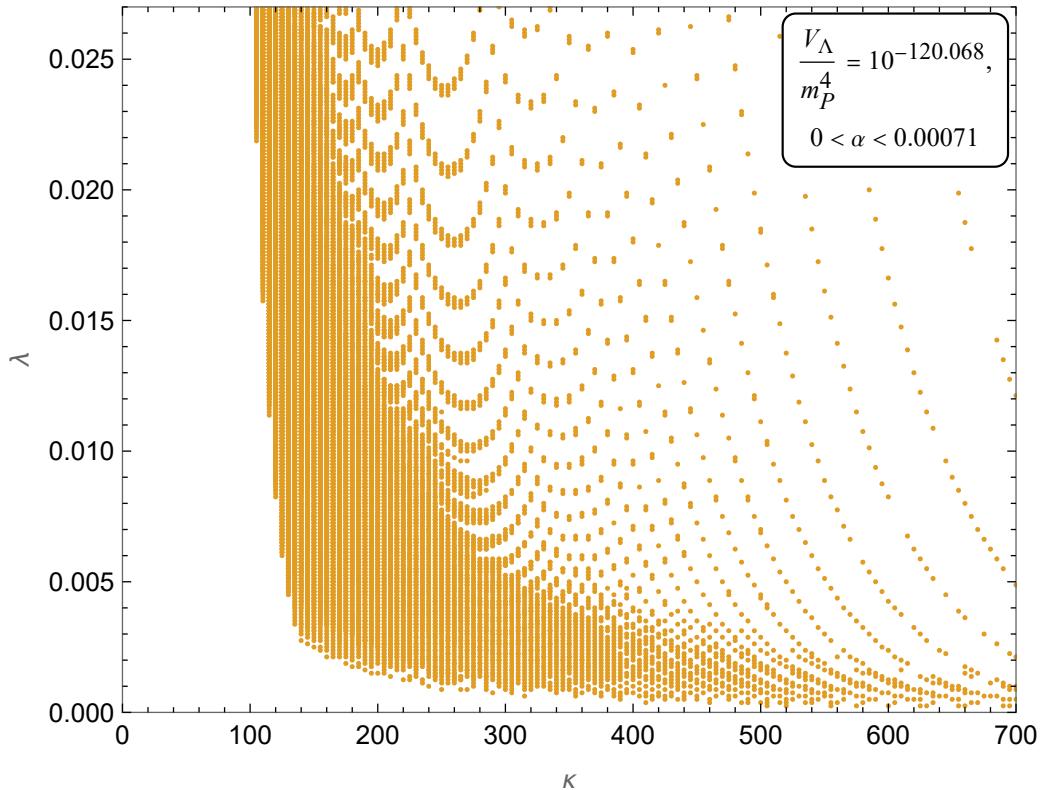


**Figure 4:** Parameter space slice in the  $\lambda - \kappa$  plane with  $0 < \alpha < 0.00071$  and  $V_\Lambda = 10^{-120.068} m_P^4$ . The orange region is constituted by the successful points, *i.e.*, those for which the constraints detailed in Table 4 are satisfied.

## 5 Initial Conditions

Our model accounts for both EDE and late-time dark energy in a non-oscillatory manner (in contrast to Ref. [34]). The field is frozen at early times, thawing just before matter-radiation equality when its density grows to nearly 0.1 of the total value (see Fig. 6), as set by constraints in Ref. [29]. A steep  $\exp(-\exp)$  potential then forces the field into free-fall, causing its energy density to dilute away as  $\rho_\phi \propto a^{-6}$ . After this, the field hits the asymptote of the exponential decay and refreezes, becoming dominant at present (see Fig. 8).

Thus, we achieve DE-like behaviour at the present day by ensuring that the field refreezes after its period of free-fall, therefore remaining at a constant energy density equal to the value of the potential density at that point. Although this constant potential density is initially negligible, the expansion of the Universe causes the density of matter to decrease. Because the field refreezes at a potential density that is comparable to the density of matter at present, the field starts to become dominant at the present day. Once it begins to dominate the Universe, the field thaws again, but the density of the Universe is dominated by a constant contribution  $V_\Lambda$ , as with  $\Lambda$ CDM.

The obvious question is why our scalar field finds itself frozen at the origin in the first place. One compelling explanation is the following. We assume that the origin is an enhanced symmetry point (ESP) such that, at very early times, an interaction of  $\varphi$  with some other scalar field  $\chi$  traps the rolling of  $\varphi$  at zero. The idea follows the scenario explored in Ref. [78].

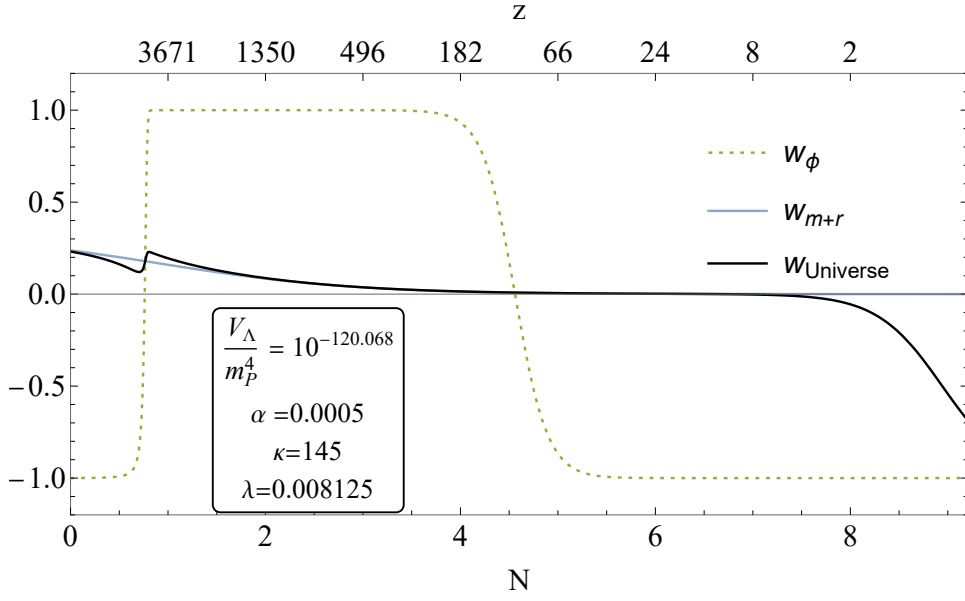


**Figure 5:** Barotropic parameter of the scalar field (dotted green), of the background perfect fluid (full blue) and of the sum of both components (full black), for  $\alpha = 0.0005$ ,  $\kappa = 145$ ,  $\lambda = 0.008125$ , and  $V_\Lambda = 10^{-120.068} m_P^4$ .

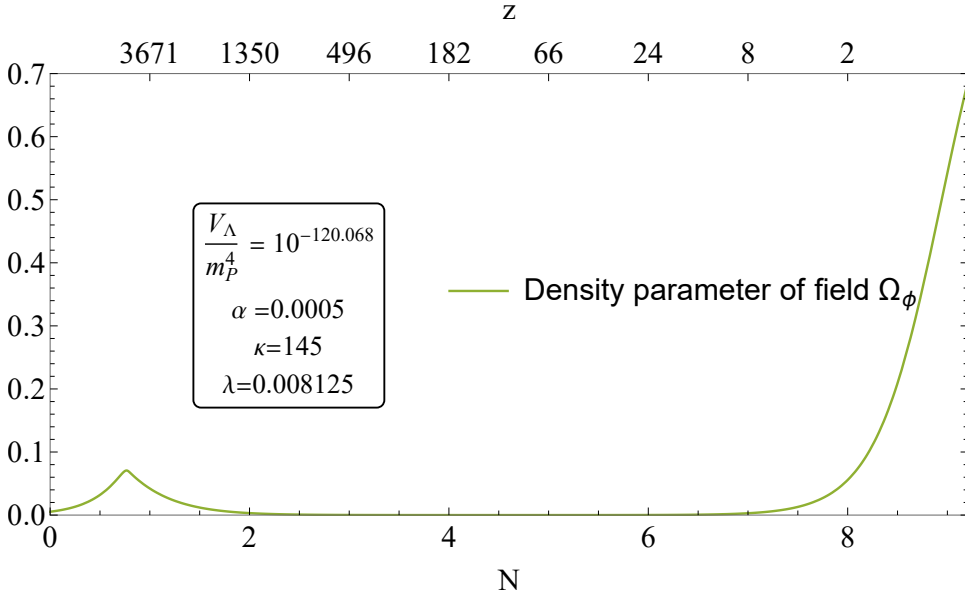


**Figure 6:** The density parameter of the scalar field, for  $\alpha = 0.0005$ ,  $\kappa = 145$ ,  $\lambda = 0.008125$ , and  $V_\Lambda = 10^{-120.068} m_P^4$ , as a function of the redshift (top) and e-folds (bottom) elapsed since the beginning of the simulation.

In this scenario, the scalar potential includes the interaction

$$\Delta V = \frac{1}{2} g^2 \varphi^2 \chi^2, \quad (5.1)$$

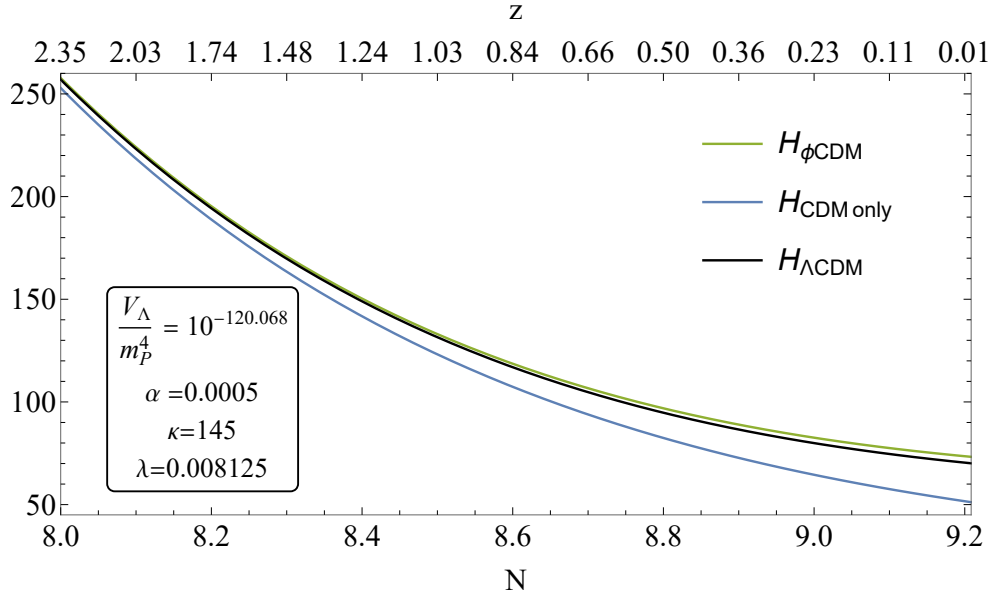


**Figure 7:** The Hubble parameter (in units of  $\text{km s}^{-1}\text{Mpc}^{-1}$ ) of a Universe with the modelled scalar field (green), a classical  $\Lambda\text{CDM}$  simulation (black), and one with only matter and radiation (blue), as a function of the redshift (top) and the e-folds (bottom) elapsed since the beginning of the simulation.

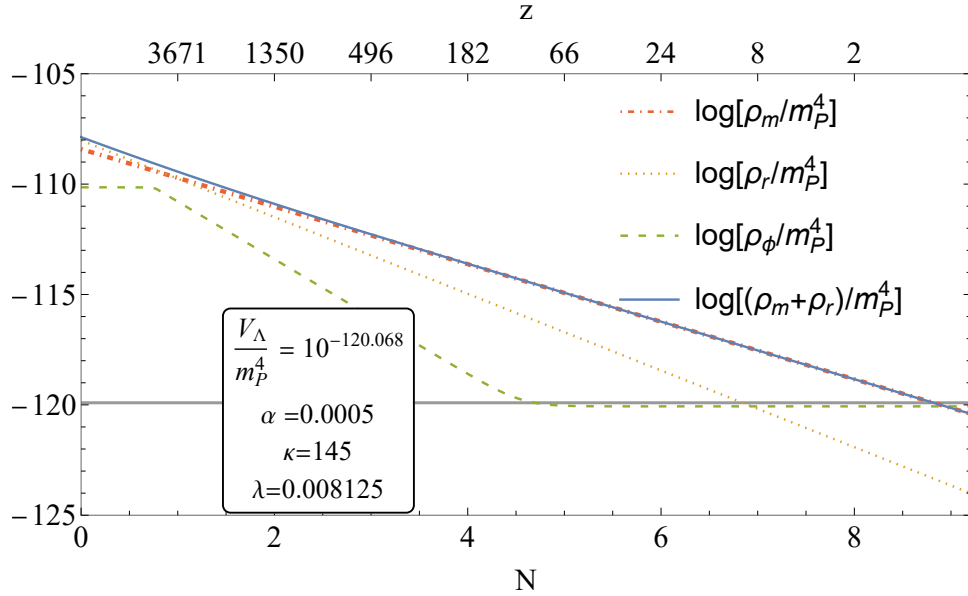


**Figure 8:** The logarithmic densities of matter (dot-dashed red), radiation (dotted orange), the sum of both (solid blue) and the scalar field (dashed green), as a function of the redshift (top) and the e-folds (bottom) elapsed since the beginning of the simulation. The horizontal full line represents the  $(SH_0\text{ES})$  energy density of the Universe at present.

where the coupling  $g < 1$  parametrises the strength of the interaction.

Constraint	Field Value
$0.015 \leq \Omega_\phi^{\text{eq}} < 0.107$	0.05178
$\Omega_\phi^{\text{ls}} < 0.015$	0.001722
$\Omega_\phi^{\text{eq}} > \Omega_\phi^{\text{ls}}$	YES
$0.6833 \leq \Omega_\phi^0 \leq 0.6945$	0.6889
$-1 \leq w_\phi^0 \leq -0.95$	-1.000
$-0.55 \leq w_\phi^a \equiv -\left.\frac{dw_\phi}{da}\right _0 \leq 0.03$	$-4.850 \times 10^{-11}$
$72.00 \leq \frac{H_0}{\text{km s}^{-1} \text{Mpc}^{-1}} \leq 74.08$	<b>73.27</b>
$\kappa\lambda$	1.178
$(\phi_0 - \phi_{\text{eq}})/m_{\text{P}} < 1$	0.4274

**Table 5:** Table giving the constraints and their corresponding values for an example point,  $\alpha = 0.0005$ ,  $\kappa = 145$ ,  $\lambda = 0.008125$ , and  $V_\Lambda$  tuned to the SH<sub>0</sub>ES cosmological constant, in the viable parameter space. The Hubble constant obtained in this example is  $H_0 = 73.27$  km/s Mpc.

We assume that initially  $\varphi$  is rolling down its steep potential.<sup>10</sup> Then, the interaction in Eq. (5.1) provides a modulated effective mass-squared  $m_{\text{eff}}^2 = g^2\varphi^2$  to the scalar field  $\chi$ . When  $\varphi$  crosses the origin, this effective mass becomes momentarily zero. If the variation of the  $\varphi$  field (i.e. the speed  $|\dot{\varphi}|$  in field space) is large enough, then there is a window around the origin when  $|\dot{m}_{\text{eff}}| \gg m_{\text{eff}}^2$  (because,  $|\dot{\varphi}| \gg \varphi^2 \simeq 0$ ). This violates adiabaticity and leads to copious production of  $\chi$ -particles [78].<sup>11</sup>

As the field moves past the ESP, the produced  $\chi$  particles become heavy, which takes more energy from the  $\varphi$  field, producing an effective potential incline in the direction the  $\varphi$  field is moving. Indeed, the particle production generates an additional linear potential  $\sim g|\varphi|n_\chi$  [78], where  $n_\chi$  is the number density of the produced  $\chi$ -particles. This number density is constant because the duration of the effect is much smaller than a Hubble time, so that we can ignore dilution from the Universe expansion. The rolling  $\varphi$  field climbs up the linear potential until its kinetic energy density is depleted. Then the field momentarily stops and afterwards reverses its motion (variation) back to the origin. When crossing the origin again, there is another bout of  $\chi$ -particle production, which increases  $n_\chi$  and makes the linear potential steeper to climb. This time,  $\varphi$  variation halts at a value closer to the origin. Then, the field reverses its motion and rushes through the origin again. Another outburst of  $\chi$ -particle production steepens the linear potential further. The process continues until the

<sup>10</sup>For away from the origin, the scalar potential  $V(\varphi)$  does not have to be of the form in Eq. (2.1). In fact, it is conceivable that  $\varphi$  might play the role of the inflaton field too (see Appendix).

<sup>11</sup>Near the origin, when  $\varphi \simeq 0$ , the  $\varphi$ -field is approximately canonically normalised, as suggested by Eq. (1.5), so the considerations of Ref. [78] are readily applicable.

$\varphi$ -field is trapped at the origin [75, 78].

The trapping of a rolling scalar field at an ESP can take place only if the  $\chi$ -particles do not decay before trapping occurs. If they did, the  $n_\chi$  would decrease and the potential  $g|\varphi|n_\chi$  would not be able to halt the motion (variation) of the  $\varphi$ -field. The end result of this process is that all the kinetic energy density of the rolling  $\varphi$  has been given to the  $\chi$ -particles. Now, since  $\varphi$  is trapped at the origin, the effective mass of the  $\chi$ -particles is zero, which means that they are relativistic matter, with density scaling as  $\rho_\chi \propto a^{-4}$ . As far as  $\varphi$  is concerned, it is trapped at the origin and its density is only  $\rho_\varphi = V(\varphi = 0) = e^{-\lambda V_X} = \text{constant}$  (cf. Eq. (2.1)).

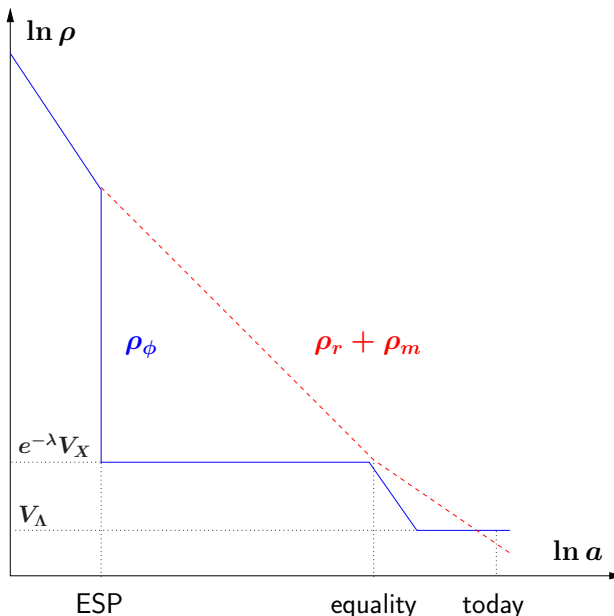


**Figure 9:** Schematic log-log plot depicting the evolution of the density of the scalar field  $\rho_\phi$  (solid blue line) and the density of radiation and matter  $\rho_r + \rho_m$  (dashed red line) in the case when the decay of the kinetic energy density of the trapped scalar field generates the thermal bath of the hot Big Bang (as in Ref. [79]). Originally the  $\phi$ -field is rushing towards the minimum of the potential, dominated by its kinetic density, so that  $\rho_\phi \propto a^{-6}$  (free-fall). When it crosses the enhanced symmetry point (ESP) its interaction to the  $\chi$ -field (cf. Eq. (5.1)) traps the rolling  $\phi$ -field at the ESP while all its kinetic energy is given to  $\chi$ -particles, which soon decay into the radiation and matter of the hot Big Bang (the decay is assumed to be quick, just after trapping). Afterwards, the  $\phi$ -field stays frozen, with energy density  $V(\phi = 0) = e^{-\lambda V_X}$  (cf. Eq. (2.1)) until much later, when its potential density is comparable to the background. Then it unfreezes before dominating, acting as early dark energy at the time near matter-radiation equality, and subsequently free-falls to its value  $\phi_0$ , with potential density approximately  $V_\Lambda = \text{constant}$ . The field stays there until the present when it dominates the Universe and becomes late dark energy.

After some time, it may be assumed that the  $\chi$ -particles do eventually decay into the standard model particles, which comprise the thermal bath of the hot Big Bang. The confining potential, which is proportional to  $n_\chi$ , disappears but, we expect the  $\varphi$ -field to remain

frozen at the origin because the scalar potential  $V(\varphi)$  in Eq. (2.1) is flat enough there. As we have discussed, the  $\varphi$ -field unfreezes again in matter-radiation equality. The above scenario is depicted in Fig. 9

For simplicity, we have considered that, apart from the obvious violation of adiabaticity at the ESP, the  $\chi$  direction is otherwise approximately flat and the  $\chi$ -field has a negligible bare mass compared to the  $\varphi$  field. It would be more realistic to consider a non-zero bare mass for the  $\chi$ -particles, which when they become non-relativistic (much later than the trapping of  $\varphi$ ) can safely decay to the thermal bath of the hot Big Bang, reheating thereby the Universe, e.g. in a manner not dissimilar to Ref. [79].

The above scenario is one possible explanation of the initial condition considered and not directly relevant to the scope of this work - numerical simulations simply assume that the field begins frozen at the origin. Other possibilities to explain our initial condition exist, for example considering a thermal correction of the form  $\delta V \propto T^2 \varphi^2$ , which would make the origin an effective minimum of the potential at high temperatures and drive the  $\varphi$ -field there.

## 6 Conclusions

In conclusion, we have studied in detail a non-oscillatory model of unified early and late dark energy, which resolves the Hubble tension and simultaneously explains the observed current accelerated expansion with no more fine tuning than  $\Lambda$ CDM. Our model considers a single scalar field in the context of  $\alpha$ -attractors, as in Ref. [34], but in our case the field is not oscillating; instead after equality, it free-falls with energy density decreasing as  $a^{-6}$ , faster than most early dark energy (EDE) proposals and the fastest possible.<sup>12</sup>

In our proposed scenario, the scalar field lies originally frozen at the origin, until it thaws near the time of equal matter-radiation densities, when it becomes EDE. Afterwards it free-falls until it refreezes at a lower potential energy density value, which provides the vacuum density of  $\Lambda$ CDM. We showed that the total excursion of the field in configuration space is sub-Planckian, which implies that our potential is stable under radiative corrections.

One explanation of our initial conditions is that the origin is an enhanced symmetry point (ESP). Our scalar field is originally kinetically dominated until it is trapped at the ESP when crossing it.<sup>13</sup> As we discuss in Appendix A, the scalar field could even be the inflaton, which after inflation rolls down its runaway potential until it becomes trapped at the ESP.

Our potential in Eq. (2.1) really serves to demonstrate that a model unifying EDE with  $\Lambda$ CDM can be achieved with a suitably steep runaway potential. With the parameters of our model assuming rather natural values, thereby not introducing fine-tuning additional to that of  $\Lambda$ CDM, we show that this is indeed possible with a simple design. The challenge lies in constructing a concrete theoretical framework for such a potential.

**Acknowledgements:** LB is supported by STFC. KD is supported (in part) by the Lancaster-Manchester-Sheffield Consortium for Fundamental Physics under STFC grant: ST/T001038/1. SSL is supported by the FST of Lancaster University.

<sup>12</sup>Causality implies that the barotropic parameter  $w$  of a perfect fluid cannot be larger than unity because the speed of sound of the fluid  $c_s^2 = w$  must be subluminal. This implies  $w \leq 1$  and so, the density of an independent perfect fluid  $\rho \propto a^{-3(1+w)}$  cannot decrease faster than  $a^{-6}$ . However, a homogeneous scalar field can be represented as a perfect fluid with  $w = \frac{\rho_{\text{kin}} - V}{\rho_{\text{kin}} + V}$ , where  $\rho_{\text{kin}}$  is the kinetic energy density of the scalar field and  $V$  the potential. It seems that  $w > 1$  could indeed happen when the field transverses an AdS minimum of  $V$ , such that  $V < 0$ . As a result, the density of such scalar field could decrease faster than  $a^{-6}$ . The scenario of such EDE has been considered in Refs. [80, 81].

<sup>13</sup>A thermal correction to the scalar potential can have a similar effect.

## A Quintessential Inflation

Is it possible that our scalar field can not only be early and late dark energy, but also be the inflaton field, responsible for accelerated expansion in the early Universe?

The  $\alpha$ -attractors construction leads to two flat regions in the scalar potential of the canonical field, as the kinetic poles of the non-canonical field are displaced to infinity. This idea has been employed in the construction of quintessential inflation models in Refs. [64–66], where the low-energy plateau was the quintessential tail, responsible for quintessence and the high-energy plateau was responsible for inflation.

However, if we inspect the potential in Eq. (2.1) at the poles  $\varphi = \pm\sqrt{6\alpha} m_{\text{P}}$ , we find that the potential for the positive pole is  $V(\varphi_+) = V_{\Lambda}$  as expected, while for the negative pole we have  $V(\varphi_-) = V_{\Lambda} \exp[2\lambda \sinh(\kappa\sqrt{6\alpha})]$ . For the values of the parameters obtained ( $\kappa \sim 10^2$ ,  $\lambda \sim 10^{-3}$  and  $\alpha \sim 10^{-4}$ ) it is easy to check that  $V(\varphi_-)$  is unsuitable for the inflationary plateau. Thus, our model needs to be modified to lead to quintessential inflation.

The first modification is a shift in field space such that our new field is

$$\tilde{\varphi} = \varphi + \Phi, \quad (\text{A.1})$$

where  $\Phi$  is a constant. The  $\alpha$ -attractors construction applies now on the new field  $\tilde{\varphi}$  for which the Lagrangian density is given by the expression in Eq. (1.4) with the substitution  $\varphi \rightarrow \tilde{\varphi}$ . The poles of our new field lie at  $\tilde{\varphi}_{\pm} = \pm\sqrt{6\tilde{\alpha}} m_{\text{P}}$ , where  $\tilde{\alpha}$  is the new  $\alpha$ -attractors parameter.

We want all our results to remain unaffected, which means that, for the positive pole, Eq. (A.1) suggests

$$\varphi_+ = \sqrt{6\alpha} m_{\text{P}} = \tilde{\varphi}_+ - \Phi = \sqrt{6\tilde{\alpha}} m_{\text{P}} - \Phi \Rightarrow \tilde{\alpha} = \frac{1}{6} \left( \frac{\Phi}{m_{\text{P}}} + \sqrt{6\alpha} \right)^2. \quad (\text{A.2})$$

The above, however, is not enough. It turns out we need to modify the scalar potential as well. This modification must be such that near the positive pole the scalar potential reduces to the one in Eq. (2.1). A simple proposal is

$$V(\tilde{\varphi}) = V_X \exp\{-2\lambda \sinh[\kappa(\tilde{\varphi} - \Phi)/m_{\text{P}}]\}, \quad (\text{A.3})$$

which indeed reduces to Eq. (2.1) when  $\kappa(\tilde{\varphi} - \Phi) = \kappa\varphi > m_{\text{P}}$ . Note that  $\kappa\sqrt{6\alpha} > 1$  is implied from the requirement that near the positive pole we have  $\kappa\sqrt{6\alpha} m_{\text{P}} = \kappa\varphi_+ > m_{\text{P}}$ . The ESP discussed in Sec. 5 is now located at  $\tilde{\varphi} = \Phi$ , such that Eq. (5.1) is now  $\Delta V = \frac{1}{2}g^2(\tilde{\varphi} - \Phi)^2\chi^2$ .<sup>14</sup>

We are interested in investigating the inflationary plateau. This is generated for the canonical field near the negative pole  $\tilde{\varphi}_- = -\sqrt{6\tilde{\alpha}} m_{\text{P}}$ , where the scalar potential of the canonical field “flattens out” [50].

Assuming that  $\Phi > \sqrt{6\alpha} m_{\text{P}}$ , we have that  $\tilde{\varphi}_- - \Phi = -2\Phi - \sqrt{6\alpha} m_{\text{P}} \simeq -2\Phi$ , where we used Eq. (A.2). Hence, for the potential energy density of the inflationary plateau we obtain

$$\begin{aligned} V_{\text{inf}} = V(\tilde{\varphi}_-) &\simeq V_X \exp[-2\lambda \sinh(-2\kappa\Phi/m_{\text{P}})] \\ &\simeq \exp\left(\lambda e^{\kappa\sqrt{6\alpha}}\right) V_{\Lambda} \exp[\lambda \exp(2\kappa\Phi/m_{\text{P}})] \\ &= \exp\left[\lambda(e^{\kappa\sqrt{6\alpha}} + e^{2\kappa\Phi/m_{\text{P}}})\right] V_{\Lambda} \simeq V_{\Lambda} \exp\left(\lambda e^{2\kappa\Phi/m_{\text{P}}}\right), \end{aligned} \quad (\text{A.4})$$

<sup>14</sup>Near the ESP the potential does not approximate Eq. (2.1). However, we assume that, after unfreezing, the field rolls away fast from the ESP, such that soon the  $\exp(\text{exp})$  form of the potential becomes valid and the evolution is the one discussed in the main text of our paper.

where we used Eq. (2.1) and that in  $-2 \sinh(-x) \simeq e^x$ , when  $x \gg 1$ .

With  $\alpha$ -attractors, the inflationary predictions are  $n_s = 1 - 2/N$  and  $r = 12\tilde{\alpha}/N^2$  [50], where  $n_s$  is the spectral index of the scalar curvature perturbation and  $r$  is the ratio of the spectrum of the tensor curvature perturbation to the spectrum of the scalar curvature perturbation, with  $N$  being the number of inflationary e-folds remaining after the cosmological scales exit the horizon. Typically,  $N = 60 - 65$  for quintessential inflation, which means that  $n_s = 0.967 - 0.969$ , in excellent agreement with the observations [82]. For the tensor-to-scalar ratio the observations provide the bound  $r < 0.036$  [83], which suggests  $\tilde{\alpha} < 0.003 N^2 = 10.8 - 12.7$ .

The COBE constraint requires  $V_{\text{inf}} \sim 10^{-10} m_{\text{P}}^4$ . Using that  $V_{\Lambda} \sim 10^{-120} m_{\text{P}}^4$ , Eq. (A.4), suggests that  $\kappa\Phi/m_{\text{P}} = \frac{1}{2} \ln(110 \ln 10/\lambda)$ . Hence, the conditions  $\Phi > \sqrt{6\alpha} m_{\text{P}}$  and  $\kappa\sqrt{6\alpha} > 1$  suggest

$$1 < \kappa\sqrt{6\alpha} < \kappa\Phi/m_{\text{P}} = \frac{1}{2} \ln(110 \ln 10/\lambda). \quad (\text{A.5})$$

Our findings in Sec. 4 are marginally in agreement with the above requirements. For example, taking  $\alpha = 0.0006$  and  $\kappa = 100$  we find  $\kappa\sqrt{6\alpha} = 6$  and then Eq. (A.5) suggests  $\lambda < 1.556 \times 10^{-3}$ . We also find  $\Phi/m_{\text{P}} > \sqrt{6\alpha} = 0.06$ , which is rather reasonable. Then, Eq. (A.2) implies  $\tilde{\alpha} > 12\alpha = 7.2 \times 10^{-3}$ , which comfortably satisfies the observational constraint on  $r$ . In fact, taking  $N \simeq 60$ , we find  $r = 12\tilde{\alpha}/N^2 > \alpha/25 = 2.4 \times 10^{-5}$ .

The above should be taken with a pinch of salt because the approximations employed are rather crude. However, they seem to suggest that our augmented model in Eq. (A.3) may lead to successful quintessential inflation while also resolving the Hubble tension, with no more fine-tuning than that of  $\Lambda$ CDM.<sup>15</sup> A full numerical investigation is needed to confirm this.

## References

- [1] **Planck** Collaboration, N. Aghanim et al., *Planck 2018 results. VI. Cosmological parameters*, *Astron. Astrophys.* **641** (2020) A6, [[arXiv:1807.06209](https://arxiv.org/abs/1807.06209)]. [Erratum: *Astron. Astrophys.* 652, C4 (2021)].
- [2] A. G. Riess et al., *A Comprehensive Measurement of the Local Value of the Hubble Constant with 1 km s<sup>-1</sup> Mpc<sup>-1</sup> Uncertainty from the Hubble Space Telescope and the SH0ES Team*, *Astrophys. J. Lett.* **934** (2022), no. 1 L7, [[arXiv:2112.04510](https://arxiv.org/abs/2112.04510)].
- [3] H. G. Escudero, J.-L. Kuo, R. E. Keeley, and K. N. Abazajian, *Early or phantom dark energy, self-interacting, extra, or massive neutrinos, primordial magnetic fields, or a curved universe: An exploration of possible solutions to the H0 and  $\sigma_8$  problems*, *Phys. Rev. D* **106** (2022), no. 10 103517, [[arXiv:2208.14435](https://arxiv.org/abs/2208.14435)].
- [4] B. S. Haridasu, H. Khoraminezhad, and M. Viel, *Scrutinizing Early Dark Energy models through CMB lensing*, [arXiv:2212.09136](https://arxiv.org/abs/2212.09136).
- [5] M. G. Dainotti, B. D. Simone, T. Schiavone, G. Montani, E. Rinaldi, and G. Lambiase, *On the hubble constant tension in the SNe ia pantheon sample*, *The Astrophysical Journal* **912** (2021), no. 2 150.
- [6] M. G. Dainotti, B. D. Simone, T. Schiavone, G. Montani, E. Rinaldi, G. Lambiase, M. Bogdan, and S. Ugale, *On the evolution of the hubble constant with the SNe ia pantheon sample and baryon acoustic oscillations: A feasibility study for GRB-cosmology in 2030*, *Galaxies* **10** (2022), no. 1 24.

---

<sup>15</sup>Unifying inflation, EDE and late DE in  $F(R)$  modified gravity has been investigated in Refs. [84, 85].

- [7] L. Knox and M. Millea, *Hubble constant hunter's guide*, *Phys. Rev. D* **101** (2020), no. 4 043533, [[arXiv:1908.03663](#)].
- [8] A. Gómez-Valent, Z. Zheng, L. Amendola, C. Wetterich, and V. Pettorino, *Coupled and uncoupled early dark energy, massive neutrinos, and the cosmological tensions*, *Phys. Rev. D* **106** (2022), no. 10 103522, [[arXiv:2207.14487](#)].
- [9] R.-G. Cai, Z.-K. Guo, S.-J. Wang, W.-W. Yu, and Y. Zhou, *No-go guide for the hubble tension: Late-time solutions*, *Physical Review D* **105** (2022), no. 2.
- [10] R.-G. Cai, Z.-K. Guo, S.-J. Wang, W.-W. Yu, and Y. Zhou, *No-go guide for late-time solutions to the hubble tension: Matter perturbations*, *Physical Review D* **106** (2022), no. 6.
- [11] T. Karwal and M. Kamionkowski, *Dark energy at early times, the Hubble parameter, and the string axiverse*, *Phys. Rev. D* **94** (2016), no. 10 103523, [[arXiv:1608.01309](#)].
- [12] V. Pettorino, L. Amendola, and C. Wetterich, *How early is early dark energy?*, *Phys. Rev. D* **87** (2013) 083009, [[arXiv:1301.5279](#)].
- [13] E. Calabrese, D. Huterer, E. V. Linder, A. Melchiorri, and L. Pagano, *Limits on dark radiation, early dark energy, and relativistic degrees of freedom*, *Physical Review D* **83** (2011), no. 12.
- [14] M. Doran and G. Robbers, *Early dark energy cosmologies*, *Journal of Cosmology and Astroparticle Physics* **2006** (2006), no. 06 026–026.
- [15] V. I. Sabla and R. R. Caldwell, *No  $H_0$  assistance from assisted quintessence*, *Phys. Rev. D* **103** (2021), no. 10 103506, [[arXiv:2103.04999](#)].
- [16] T. L. Smith, V. Poulin, and M. A. Amin, *Oscillating scalar fields and the Hubble tension: a resolution with novel signatures*, *Phys. Rev. D* **101** (2020), no. 6 063523, [[arXiv:1908.06995](#)].
- [17] K. Murai, F. Naokawa, T. Namikawa, and E. Komatsu, *Isotropic cosmic birefringence from early dark energy*, [[arXiv:2209.07804](#)].
- [18] L. M. Capparelli, R. R. Caldwell, and A. Melchiorri, *Cosmic birefringence test of the Hubble tension*, *Phys. Rev. D* **101** (2020), no. 12 123529, [[arXiv:1909.04621](#)].
- [19] K. V. Berghaus and T. Karwal, *Thermal Friction as a Solution to the Hubble and Large-Scale Structure Tensions*, [[arXiv:2204.09133](#)].
- [20] K. V. Berghaus and T. Karwal, *Thermal Friction as a Solution to the Hubble Tension*, *Phys. Rev. D* **101** (2020), no. 8 083537, [[arXiv:1911.06281](#)].
- [21] J. Sakstein and M. Trodden, *Early Dark Energy from Massive Neutrinos as a Natural Resolution of the Hubble Tension*, *Phys. Rev. Lett.* **124** (2020), no. 16 161301, [[arXiv:1911.11760](#)].
- [22] T. Karwal, M. Raveri, B. Jain, J. Khoury, and M. Trodden, *Chameleon early dark energy and the Hubble tension*, *Phys. Rev. D* **105** (2022), no. 6 063535, [[arXiv:2106.13290](#)].
- [23] V. I. Sabla and R. R. Caldwell, *Microphysics of early dark energy*, *Phys. Rev. D* **106** (2022), no. 6 063526, [[arXiv:2202.08291](#)].
- [24] M.-X. Lin, G. Benevento, W. Hu, and M. Raveri, *Acoustic Dark Energy: Potential Conversion of the Hubble Tension*, *Phys. Rev. D* **100** (2019), no. 6 063542, [[arXiv:1905.12618](#)].
- [25] E. McDonough and M. Scalisi, *Towards Early Dark Energy in String Theory*, [[arXiv:2209.00011](#)].
- [26] V. Poulin, T. L. Smith, D. Grin, T. Karwal, and M. Kamionkowski, *Cosmological implications of ultralight axionlike fields*, *Phys. Rev. D* **98** (2018), no. 8 083525, [[arXiv:1806.10608](#)].
- [27] F. Niedermann and M. S. Sloth, *Resolving the Hubble tension with new early dark energy*, *Phys. Rev. D* **102** (2020), no. 6 063527, [[arXiv:2006.06686](#)].

- [28] J. C. Hill, E. McDonough, M. W. Toomey, and S. Alexander, *Early dark energy does not restore cosmological concordance*, *Phys. Rev. D* **102** (2020), no. 4 043507, [[arXiv:2003.07355](#)].
- [29] T. L. Smith, V. Poulin, J. L. Bernal, K. K. Boddy, M. Kamionkowski, and R. Murgia, *Early dark energy is not excluded by current large-scale structure data*, *Phys. Rev. D* **103** (2021), no. 12 123542, [[arXiv:2009.10740](#)].
- [30] S. Nojiri, S. D. Odintsov, D. Saez-Chillon Gomez, and G. S. Sharov, *Modeling and testing the equation of state for (Early) dark energy*, *Phys. Dark Univ.* **32** (2021) 100837, [[arXiv:2103.05304](#)].
- [31] V. Poulin, T. L. Smith, T. Karwal, and M. Kamionkowski, *Early Dark Energy Can Resolve The Hubble Tension*, *Phys. Rev. Lett.* **122** (2019), no. 22 221301, [[arXiv:1811.04083](#)].
- [32] K. Freese and M. W. Winkler, *Chain early dark energy: A Proposal for solving the Hubble tension and explaining today’s dark energy*, *Phys. Rev. D* **104** (2021), no. 8 083533, [[arXiv:2102.13655](#)].
- [33] P. Agrawal, F.-Y. Cyr-Racine, D. Pinner, and L. Randall, *Rock ‘n’ Roll Solutions to the Hubble Tension*, [arXiv:1904.01016](#).
- [34] M. Braglia, W. T. Emond, F. Finelli, A. E. Gumrukcuoglu, and K. Koyama, *Unified framework for early dark energy from  $\alpha$ -attractors*, *Phys. Rev. D* **102** (2020), no. 8 083513, [[arXiv:2005.14053](#)].
- [35] H. Moshafi, H. Firouzjahi, and A. Talebian, *Multiple Transitions in Vacuum Dark Energy and  $H_0$  Tension*, *Astrophys. J.* **940** (2022), no. 2 121, [[arXiv:2208.05583](#)].
- [36] E. Guendelman, R. Herrera, and D. Benisty, *Unifying inflation with early and late dark energy with multiple fields: Spontaneously broken scale invariant two measures theory*, *Phys. Rev. D* **105** (2022), no. 12 124035, [[arXiv:2201.06470](#)].
- [37] O. Seto and Y. Toda, *Comparing early dark energy and extra radiation solutions to the hubble tension with bbn*, *Phys. Rev. D* **103** (2021) 123501.
- [38] S. Vagnozzi, *New physics in light of the  $h_0$  tension: An alternative view*, *Physical Review D* **102** (2020), no. 2.
- [39] A. Reeves, L. Herold, S. Vagnozzi, B. D. Sherwin, and E. G. M. Ferreira, *Restoring cosmological concordance with early dark energy and massive neutrinos?*, .
- [40] H. M. Sadjadi and V. Anari, *Early dark energy and the screening mechanism*, .
- [41] **BOSS** Collaboration, S. Alam et al., *The clustering of galaxies in the completed SDSS-III Baryon Oscillation Spectroscopic Survey: cosmological analysis of the DR12 galaxy sample*, *Mon. Not. Roy. Astron. Soc.* **470** (2017), no. 3 2617–2652, [[arXiv:1607.03155](#)].
- [42] **Planck** Collaboration, P. A. R. Ade et al., *Planck 2013 results. XVI. Cosmological parameters*, *Astron. Astrophys.* **571** (2014) A16, [[arXiv:1303.5076](#)].
- [43] R. de Sá, M. Benetti, and L. L. Graef, *An empirical investigation into cosmological tensions*, *Eur. Phys. J. Plus* **137** (2022), no. 10 1129, [[arXiv:2209.11476](#)].
- [44] S. Vagnozzi, *Consistency tests of  $\lambda$ cdm from the early integrated sachs-wolfe effect: Implications for early-time new physics and the hubble tension*, *Physical Review D* **104** (2021), no. 6.
- [45] R. C. Nunes and S. Vagnozzi, *Arbitrating the  $s_8$  discrepancy with growth rate measurements from redshift-space distortions*, *Monthly Notices of the Royal Astronomical Society* **505** (jun, 2021) 5427–5437.
- [46] R. Kallosh and A. Linde, *Universality Class in Conformal Inflation*, *JCAP* **07** (2013) 002, [[arXiv:1306.5220](#)].
- [47] A. Linde, D.-G. Wang, Y. Welling, Y. Yamada, and A. Achúcarro, *Hypernatural inflation*, *JCAP* **07** (2018) 035, [[arXiv:1803.09911](#)].

- [48] R. Kallosh and A. Linde, *Planck, LHC, and  $\alpha$ -attractors*, *Phys. Rev. D* **91** (2015) 083528, [[arXiv:1502.07733](#)].
- [49] S. Cecotti and R. Kallosh, *Cosmological Attractor Models and Higher Curvature Supergravity*, *JHEP* **05** (2014) 114, [[arXiv:1403.2932](#)].
- [50] R. Kallosh, A. Linde, and D. Roest, *Superconformal Inflationary  $\alpha$ -Attractors*, *JHEP* **11** (2013) 198, [[arXiv:1311.0472](#)].
- [51] S. Ferrara, R. Kallosh, A. Linde, and M. Porrati, *Minimal Supergravity Models of Inflation*, *Phys. Rev. D* **88** (2013), no. 8 085038, [[arXiv:1307.7696](#)].
- [52] S. Ferrara, P. Fré, and A. S. Sorin, *On the Topology of the Inflaton Field in Minimal Supergravity Models*, *JHEP* **04** (2014) 095, [[arXiv:1311.5059](#)].
- [53] S. Ferrara, P. Fre, and A. S. Sorin, *On the Gauged Kähler Isometry in Minimal Supergravity Models of Inflation*, *Fortsch. Phys.* **62** (2014) 277–349, [[arXiv:1401.1201](#)].
- [54] R. Kallosh, A. Linde, and D. Roest, *Large field inflation and double  $\alpha$ -attractors*, *JHEP* **08** (2014) 052, [[arXiv:1405.3646](#)].
- [55] A. Linde, *Does the first chaotic inflation model in supergravity provide the best fit to the Planck data?*, *JCAP* **02** (2015) 030, [[arXiv:1412.7111](#)].
- [56] A. A. Starobinsky, *A New Type of Isotropic Cosmological Models Without Singularity*, *Phys. Lett. B* **91** (1980) 99–102.
- [57] F. L. Bezrukov and M. Shaposhnikov, *The Standard Model Higgs boson as the inflaton*, *Phys. Lett. B* **659** (2008) 703–706, [[arXiv:0710.3755](#)].
- [58] A. Alho and C. Ugla, *Inflationary  $\alpha$ -attractor cosmology: A global dynamical systems perspective*, *Phys. Rev. D* **95** (2017), no. 8 083517, [[arXiv:1702.00306](#)].
- [59] S. D. Odintsov and V. K. Oikonomou, *Inflationary  $\alpha$ -attractors from  $F(R)$  gravity*, *Phys. Rev. D* **94** (2016), no. 12 124026, [[arXiv:1612.01126](#)].
- [60] M. Braglia, A. Linde, R. Kallosh, and F. Finelli, *Hybrid  $\alpha$ -attractors, primordial black holes and gravitational wave backgrounds*, [[arXiv:2211.14262](#)].
- [61] R. Kallosh and A. Linde, *Hybrid cosmological attractors*, *Phys. Rev. D* **106** (2022), no. 2 023522, [[arXiv:2204.02425](#)].
- [62] A. Achúcarro, R. Kallosh, A. Linde, D.-G. Wang, and Y. Welling, *Universality of multi-field  $\alpha$ -attractors*, *JCAP* **04** (2018) 028, [[arXiv:1711.09478](#)].
- [63] O. Iarygina, E. I. Sfakianakis, D.-G. Wang, and A. Achúcarro, *Multi-field inflation and preheating in asymmetric  $\alpha$ -attractors*, [[arXiv:2005.00528](#)].
- [64] Y. Akrami, R. Kallosh, A. Linde, and V. Vardanyan, *Dark energy,  $\alpha$ -attractors, and large-scale structure surveys*, *JCAP* **06** (2018) 041, [[arXiv:1712.09693](#)].
- [65] K. Dimopoulos, L. Donaldson Wood, and C. Owen, *Instant preheating in quintessential inflation with  $\alpha$ -attractors*, *Phys. Rev. D* **97** (2018), no. 6 063525, [[arXiv:1712.01760](#)].
- [66] K. Dimopoulos and C. Owen, *Quintessential Inflation with  $\alpha$ -attractors*, *JCAP* **06** (2017) 027, [[arXiv:1703.00305](#)].
- [67] **Supernova Search Team** Collaboration, A. G. Riess et al., *Observational evidence from supernovae for an accelerating universe and a cosmological constant*, *Astron. J.* **116** (1998) 1009–1038, [[astro-ph/9805201](#)].
- [68] R. R. Caldwell, R. Dave, and P. J. Steinhardt, *Cosmological imprint of an energy component with general equation of state*, *Phys. Rev. Lett.* **80** (1998) 1582–1585, [[astro-ph/9708069](#)].
- [69] M. Chevallier and D. Polarski, *Accelerating universes with scaling dark matter*, *Int. J. Mod. Phys. D* **10** (2001) 213–224, [[gr-qc/0009008](#)].

- [70] E. V. Linder, *Exploring the expansion history of the universe*, *Phys. Rev. Lett.* **90** (2003) 091301, [[astro-ph/0208512](#)].
- [71] A. Banerjee, H. Cai, L. Heisenberg, E. O. Colgáin, M. M. Sheikh-Jabbari, and T. Yang, *Hubble sinks in the low-redshift swampland*, *Phys. Rev. D* **103** (2021), no. 8 L081305, [[arXiv:2006.00244](#)].
- [72] B.-H. Lee, W. Lee, E. O. Colgáin, M. M. Sheikh-Jabbari, and S. Thakur, *Is local  $H_0$  at odds with dark energy EFT?*, *JCAP* **04** (2022), no. 04 004, [[arXiv:2202.03906](#)].
- [73] E. J. Copeland, A. R. Liddle, and D. Wands, *Exponential potentials and cosmological scaling solutions*, *Phys. Rev. D* **57** (1998) 4686–4690, [[gr-qc/9711068](#)].
- [74] E. J. Copeland, M. Sami, and S. Tsujikawa, *Dynamics of dark energy*, *Int. J. Mod. Phys. D* **15** (2006) 1753–1936, [[hep-th/0603057](#)].
- [75] K. Dimopoulos, *Introduction to Cosmic Inflation and Dark Energy*. CRC Press, 5, 2022.
- [76] G. B. Gelmini, *Cosmology and astroparticles*, in *AIP Conference Proceedings*, AIP, 1996.
- [77] D. Wands, O. F. Piattella, and L. Casarini, *Physics of the cosmic microwave background radiation*, in *The Cosmic Microwave Background*, pp. 3–39. Springer International Publishing, 2016.
- [78] L. Kofman, A. D. Linde, X. Liu, A. Maloney, L. McAllister, and E. Silverstein, *Beauty is attractive: Moduli trapping at enhanced symmetry points*, *JHEP* **05** (2004) 030, [[hep-th/0403001](#)].
- [79] K. Dimopoulos, M. Karčiauskas, and C. Owen, *Quintessential inflation with a trap and axionic dark matter*, *Phys. Rev. D* **100** (2019), no. 8 083530, [[arXiv:1907.04676](#)].
- [80] G. Ye and Y.-S. Piao, *Is the Hubble tension a hint of AdS phase around recombination?*, *Phys. Rev. D* **101** (2020), no. 8 083507, [[arXiv:2001.02451](#)].
- [81] G. Ye and Y.-S. Piao,  *$T_0$  censorship of early dark energy and AdS vacua*, *Phys. Rev. D* **102** (2020), no. 8 083523, [[arXiv:2008.10832](#)].
- [82] **Planck** Collaboration, Y. Akrami et al., *Planck 2018 results. X. Constraints on inflation*, *Astron. Astrophys.* **641** (2020) A10, [[arXiv:1807.06211](#)].
- [83] **BICEP, Keck** Collaboration, P. A. R. Ade et al., *Improved Constraints on Primordial Gravitational Waves using Planck, WMAP, and BICEP/Keck Observations through the 2018 Observing Season*, *Phys. Rev. Lett.* **127** (2021), no. 15 151301, [[arXiv:2110.00483](#)].
- [84] S. Nojiri, S. D. Odintsov, and V. K. Oikonomou, *Unifying Inflation with Early and Late-time Dark Energy in  $F(R)$  Gravity*, *Phys. Dark Univ.* **29** (2020) 100602, [[arXiv:1912.13128](#)].
- [85] V. K. Oikonomou, *Unifying inflation with early and late dark energy epochs in axion  $F(R)$  gravity*, *Phys. Rev. D* **103** (2021), no. 4 044036, [[arXiv:2012.00586](#)].